Published in final edited form as:
*Neuroimage*. 2010 June ; 51(2): 623–628. doi:10.1016/j.neuroimage.2010.02.015.

# Effects of Low-Field Magnetic Stimulation on Brain Glucose Metabolism

**Nora D. Volkow, M.D.**[1,2,*], **Dardo Tomasi, Ph.D.**[2], **Gene-Jack Wang, M.D.**[3], **Joanna S. Fowler, Ph.D.**[3], **Frank Telang, M.D.**[2], **Ruiliang Wang, Ph.D.**[3], **Dave Alexoff, PhD.**[3], **Jean Logan, Ph.D.**[3], **Christopher Wong, M.S.**[3], **Kith Pradhan, M.S.**[3], **Elisabeth C. Caparelli, Ph.D.**[3], **Yeming Ma, Ph.D.**[2], and **Millard Jayne, R.N.**[2]

[1]National Institute on Drug Abuse, Bethesda MD 20892

[2]National Institute on Alcohol Abuse and Alcoholism, Bethesda MD 20892

[3]Medical Department, Brookhaven National Laboratory, Upton NY 11973

## Abstract

Echo Planar imaging (EPI), the gold standard technique for functional MRI (fMRI), is based on fast magnetic field gradient switching. These time-varying magnetic fields induce electric (E) fields in the brain that could influence neuronal activity; but this has not been tested. Here we assessed the effects of EPI on brain glucose metabolism (marker of brain function) using PET and 18F 2-fluoro-2-deoxy-D-glucose ($^{18}$FDG). Fifteen healthy subjects were in a 4 T magnet during the $^{18}$FDG uptake period twice: with (ON) and without (OFF) EPI gradients pulses along the *z*-axis ($G_z$: 23 mT/m; 250 microsecond rise-time; 920 Hz). The E-field from these EPI pulses is non-homogeneous, increasing linearly from the gradient's isocenter (radial and z directions), which allowed us to assess the correlation between local strength of the E-field and the regional metabolic differences between ON and OFF sessions. Metabolic images were normalized to metabolic activity in the plane positioned at the gradient's isocenter where E=0 for both ON and OFF conditions. Statistical parametric analyses used to identify regions that differed between ON versus OFF ($p<0.05$, corrected) showed that the relative metabolism was lower in areas at the poles of the brain (inferior occipital and frontal and superior parietal cortices) for ON than for OFF, which was also documented with individual region of interest analysis. Moreover the magnitude of the metabolic decrements was significantly correlated with the estimated strength of E ($r=0.68$, $p<0.0001$); the stronger the E-field the larger the decreases. However, we did not detect differences between ON versus OFF conditions on mood ratings nor on absolute whole brain metabolism. This data provides preliminary evidence that EPI sequences may affect neuronal activity and merits further investigation.

### Keywords

brain imaging; echo planar; brain glucose metabolism; fMRI

Functional MRI (fMRI), which non-invasively measures dynamic MRI signal changes using the blood-oxygenation level dependent (BOLD) contrast, has become an indispensable tool to

*Correspondence: Nora D. Volkow, M.D., National Institute on Drug Abuse, 6001 Executive Boulevard, Room 5274, MSC 9581, Bethesda, MD 20892, Tel. (301)443-6480, Fax (301)443-9127, nvolkow@nida.nih.gov.

investigate human brain function (Fox and Raichle, 2007). Echo Planar imaging (EPI) is the gold standard technique for fMRI and it is based on the use of fast switching of magnetic field gradients, which are superimposed to the static magnetic field of the MRI instrument (Stehling et al., 1991). However, the potential influence of the magnetic fields (static and time-varying) on brain function is a concern for fMRI studies (Kangarlu et al., 1999). Using PET and $^{18}$FDG to measure brain glucose metabolism (marker of brain function) (Sokoloff et al., 1977), we had shown that the static magnetic field of a human MRI instrument (4 Tesla) did not affect brain glucose metabolism (Volkow et al., 2000), which suggests that the static magnetic field does not modify brain activity significantly. However, whereas static magnetic fields do not induce electric currents, varying magnetic fields do (Jackson, 1975), and the induction of such electric current in the brain could influence neuronal activity (Walsh and Rushworth, 1999; Crasson et al., 1999). Indeed, transcranial magnetic stimulation (TMS), which uses time-varying magnetic fields to affect neuronal brain activity (Brestmann, 2008) is used in research as a tool to investigate brain function (Paus, 2005) and in the clinic for therapeutic purposes (repeated TMS) including its use for the treatment of depression (Gershon et al., 2003). Moreover, EPI sequences typical of MRI were recently shown to have “antidepressant like” effects in laboratory animals (forced swimming test) (Rokni-Yasdi et al., 2007; Aksoz et al., 2008) and to improve mood in depressed patients (Rohan et al., 2004). This would suggest that EPI may affect neuronal activity even though the induced E-fields are much weaker than those induced by TMS (1 v 100 V/m respectively) (Speer et al., 2000). Since EPI is being increasingly utilized to study human brain function (Dolan, 2008; Rosen et al., 1998; Harel et al., 2006), it is important to assess any effects there from.

Here we used PET and $^{18}$FDG to test if there were effects of EPI on brain glucose metabolism. For this purpose we measured brain glucose metabolism in fifteen healthy subjects twice while their heads were in a 4 T MRI instrument during the uptake period of $^{18}$FDG; once with EPI readout gradient pulses along the *z*-axis ON and once with EPI gradient pulses OFF but with the simulated noise from the gradients; after which they were scanned in the PET scanner (Figure 1). Because metabolic activity as assessed with $^{18}$FDG mostly reflects the uptake period of $^{18}$FDG into the brain (Sokoloff et al., 1977;Reivich et al., 1979), this allowed us to assess the effects of the EPI readout gradient on resting brain metabolism while they were in the magnet. Since both low intensity TMS pulses (Todd et al., 2006) and paired TMS pulses with short-intervals (1–4 ms) are inhibitory (Ziemann et al., 1996), we hypothesized that EPI would decrease metabolic activity, due to the low intensity of the E-fields and the short-interval between readout gradient pulses (1ms) used in EPI. We further hypothesized that using a coronal orientation with readout along *z*, the decreases would be proportional to the distance from isocenter ($z = 0$) due to the anti-symmetric and linear nature of the E-field induced by the *z*-gradient (Glover and Bowtell, 2007).

## MATERIALS AND METHODS

### Subjects

We studied 15 healthy right-handed males (33 ±7 years of age) who responded to an advertisement. Subjects were initially screened by phone and then evaluated at Brookhaven National Laboratory by a physician for exclusion criteria, which included current or past psychiatric disorder (including drug abuse or dependence), neurological disease, significant medical illness, current treatment with medication (including over the counter drugs) and pregnancy. Normal physical examination and laboratory tests were required for entry. Pre-scan urine tests ensured the absence of any psychoactive drugs. Subjects were monetarily compensated for their participation. Written informed consent was obtained in all subjects in accordance with the local Institutional Review Board.

### Behavioral measures

Emotional affectivity was assessed using the Positive and Negative Affect Schedule (PANAS) (Watson et al., 1988). The questionnaire consists of 20 descriptors of either positive or negative mood states (ranked from 1 to 5). The PANAS was completed by the subjects before getting into the MRI and at the end of the EPI or the Sham Stimulation conditions (see below).

### PET Scan and FDG Uptake Conditions

All subjects underwent two PET $^{18}$FDG scans to measure brain metabolism while inside the MRI scanner; one day with EPI gradients ON and another day with EPI gradients OFF (Sham condition). The order of the ON and Sham conditions was randomly assigned and subjects did not know the order of the sessions. The subjects' head was positioned within the head RF-coil with ear protection (earplugs and headphones) to minimize auditory stimulation. A sagittal T1 weighted image was used to locate the upper portion of the corpus callosum, which was placed at the isocenter (z= 0; where E = 0) of the SONATA/Siemens gradient set of the 4-Tesla Varian MRI scanner. Subjects had two venous catheters placed; one for radiotracer injection and one for venous blood sampling. The subjects were injected with $^{18}$FDG (4–6 mCi) 20-minutes after their entrance in the magnet. They were asked to refrain from moving or speaking during the 25-minute $^{18}$FDG uptake period and were requested to keep their eyes open to monitor that they did not fall asleep. Five minutes after $^{18}$FDG injection the subjects were removed from the scanner for one minute to take a blood sample and placed back in position in the MRI scanner (corpus callosum at isocenter); they remained in the MRI table with their heads in the RF coil and were told to refrain from moving. We computed glucose metabolic rates using a simplified method that relies on two-point blood sampling (5 and 35 minutes post FDG injection) as previously described (Logan et al., 2008). Briefly, for the estimation of the metabolic rate we used the following rate constants: $K_1$=0.1 ml/min/g and $k_2$+$k_3$=0.2 min$^{-1}$ and for the Lumped Constant (LC) = 0.50 (Books et al., 1987). The two-point blood sampling method was validated by comparing the metabolic rates with those obtained from 100 FDG images for which metabolic rates were also quantified using the complete set of arterialized blood samples and showed that the average correlation between these two methods was 0.93 ±0.08 (Logan et al., 2008).

During the ON session, a standard blipped gradient echo EPI pulse sequence (TE/TR = 20/1600 ms, 4-mm slice thickness, 35 coronal slices) without RF pulses was used to stimulate the subject's brain continuously during the 15 minutes prior to and during the 25 minutes after $^{18}$FDG injection (uptake period). The EPI readout gradient waveform was delivered by the longitudinal $G_z$-coil and formed by a train of 64 alternating trapezoids of amplitude = 23 mT/m, rise time = 0.25 ms, and duration = 0.543 ms (Figure 2). Note the root mean square amplitude of the *E*-field induced by the EPI readout gradient is 100 times or higher than that induced by the phase encoding and slice select gradients. While the transverse gradient coils, $G_x$ and $G_y$, induce highly uniform **E** along the *y*- and *x*-axes, respectively (Rohan et al., 2004), the longitudinal gradient coil $G_z$ induces an azimuthal $\mathbf{E} = E\hat{\boldsymbol{\phi}}$ which is anti-symmetrical with respect to the $z = 0$ plane and its amplitude can be approximated as (Glover and Bowtell, 2007):

$$\mathbf{E}(r,z,t)=\frac{rz}{2}\left(\frac{dG_z(t)}{dt}\right)\widehat{\phi}$$

where *r* is the radial distance to magnet axis and *t* is the time. Therefore, the amplitude of the electric field induced by $G_z$ is null at the $z = 0$ plane and at the $r = 0$ axis and increases linearly with *r* and *z*, and it is further modulated by the temporal derivative of $G_z$, an alternating square

waveform with amplitude proportional to the slew-rate of the trapezoidal gradient (Rohan et al., 2004).

During the Sham session (EPI OFF), the EPI gradient pulses were replaced by the sound of the EPI sequence (64 dBA = EPI sound pressure level at the subjects' ears after the 28 dBA of sound attenuation provided by the headphones), which was recorded in waveform audio format in a PC and delivered to the subjects' ears through the headphones.

At the end of the sessions, the subjects were removed from the MRI scanner and were positioned in the PET scanner as previously described (Wang et al., 1993). Subjects were scanned with a whole-body, high-resolution tomograph (Siemens/CTI ECAT HR+, with 4.6 × 4.6 × 4.2 $mm^3$ NEMA (National Electrical Manufacturers Association). Briefly, emission scans started 35 minutes after $^{18}$FDG injection (10 minutes after being taken out of the MRI scanner) and lasted twenty minutes. Transmission scans were performed simultaneously. Because the subjects were inside the magnet during the $^{18}$FDG uptake period we were unable to quantify arterialized plasma concentration to compute the absolute metabolic images and thus images were quantified by normalizing them to the axial plane at the isocenter of the EPI gradients, which is where E = 0. Figure 1 provides a diagram of the experimental procedure.

## Estimation of the Electric Fields in Brain

The distribution of current carrying wires in the $G_z$-gradient coil was estimated from the physical dimensions (primary radius: 0.7m; shielding radius: 0.84m; and coil length: 0.8m) and electrical parameters (gradient efficiency: 0.08 mT/m/A; maximum gradient strength: 40mT/m; coil inductance: 1.1mH) of typical EPI gradient coils using the stream function optimization method (Tomasi, 2001). The theory of classical electromagnetism [reviewed in (Jackson, 1975)] was used to compute **E** for each point in space as the temporal derivative of the vector potential produced by the current distribution in the coil (Cronik and Rutt, 2001; Tomasi et al., 2002).

## Image Analysis

The statistical parametric mapping package SPM2 (Welcome Department of Cognitive Neurology, London UK) (Friston, 1995) was used to compare the differences between the two conditions. For this purpose images were spatially normalized using the SPM2 PET template using a 2 × 2 × 2 $mm^3$ voxel size, and subsequently smoothed with an 8-mm isotropic Gaussian kernel. The metabolic activity in each imaging voxel was then normalized to the average metabolic activity in the **E** = 0 plane (middle axial plane that includes the upper part of the corpus callosum and was at the isocenter of the EPI gradients during stimulation). This allowed us to normalize brain metabolism using an area of the brain where the *E*-field did not differ between EPI and Sham stimulation conditions. Voxel-wise paired samples *t*-tests were performed to contrast the EPI versus the Sham conditions. The continuous random field calculation implemented in SPM2 was used to correct the statistical significance of normalized metabolic changes ($\Delta^{18}$FDG), for multiple comparisons at the cluster level. Clusters with at least 20 voxels (voxel size 2×2×2 $mm^3$) and $p < 0.05$ (corrected for multiple comparisons) were considered significant. These clusters were further evaluated with region-of-interest (ROI) analyses to obtain average signal values in a volume comparable to the image smoothness (e.g. resolution elements, or "resels" (Worsley et al., 1992)) rather than single-voxel peak values. The volume of the imaging resels obtained from the SPM analysis was near cubic with a Cartesian full-width-half-maximum (FWHM) = 13.9 mm, 15.6 mm, 18.3 mm. Thus, 6×6×6 $mm^3$ isotropic masks (0.22 ml) were defined at the centers of relevant clusters listed in Table 1 to extract the average glucose metabolism from individual contrast maps. The average and standard deviation of metabolic values within these regions were computed using a custom program written in IDL (ITT Visual Information Solutions, Boulder, CO). The coordinates of

the functional ROI masks were kept fixed across subjects, and paired t test were used to assess statistical significance.

Regression analyses were used to test the hypothesis of a linear relationship between FDG decreases (ΔFDG) and *E*. The paired ($\Delta FDG_i$, $E_i$) values from all subjects and voxels in the brain were sorted by *E* and clustered in groups of 100 subsequent voxels. The data within these clusters was averaged and a linear model, $\Delta FDG = a\,E + b$, was fitted to the averaged clusters to assess the linear relationship between ΔFDG and *E*.

## RESULTS

Estimation of the **E**-field in the brain revealed that the strength of **E** was maximal at the poles (top and bottom) and in the posterior parts of the brain; the latter reflecting the fact that the center of the head (center of the Talairach stereotactic space where xyz = 0,0,0 mm) was 2.0 ± 0.5 cm below the gradient isocenter and thus posterior regions were closer to the wires and thus experienced higher E-fields than anterior regions (Figure 3).

There were no differences on whole brain glucose metabolism between the ON (27 ±4 μmol/100g/min) and OFF (28 ±5 μmol/100g/min) conditions. The SPM analyses on the normalized metabolic images (to plane E =0) revealed significant ($p < 0.05$, corrected for multiple comparisons) decreases in 7 cluster areas that included inferior occipital, inferior frontal, superior parietal and posterior insular cortices and in a white matter region contiguous to the temporal cortex (Figure 4, Table 1). None of the brain regions showing increases with EPI ON when compared with Sham achieved significance. Separate region of interest (ROI) analysis that quantified relative metabolic changes in the anatomical regions identified by SPM documented significant decreases in inferior occipital (BA 18), inferior frontal (BA 8, BA 11) and superior parietal cortices (BA 40) but the differences in posterior insula and white matter were not significant (Table 1).

The correlation between the relative metabolic changes (expressed as percent change from the Sham condition) and the strength of **E** was significant ($r = 0.68$, $p < 0.0001$) (Figure 5); the stronger the local *E*-field the higher the decreases in metabolism with EPI ON.

The scores on mood (positive scale from the PANAS) did not change on the measures done before (40 ±7) and those done after (40 ±8) the EPI OFF condition nor did they differ for the measures done before (39 ±8) and after (40 ±9) the EPI ON condition.

## DISCUSSION

Here we show that while the electrical fields induced during EP MRI did not change the absolute whole brain metabolic rate it induced small but significant changes in normalized metabolic measures. Specifically we showed significant reductions in relative metabolic measures in superior, inferior and posterior cortical regions with the EPI Gradients ON when compared with EPI gradients OFF, which provides preliminary evidence that EPI as used in fMRI studies may affect neuronal activity in the human brain. The regional localization of these metabolic changes would indicate that the effects of EPI on brain activity are non-homogeneous and dependent on the local *E*-field. The correlations observed between the magnitude of the metabolic changes and **E** suggests that the metabolic decreases may be causally associated with the changes in **E** produced by the magnetic fields gradients. These results are consistent with prior studies showing that fluctuating magnetic fields can influence brain activity (Walsh and Rushworth, 1999; Crasson et al., 1999) and contrasts with findings failing to show an effect of static magnetic fields on brain glucose metabolism (4 T MR) (Volkow et al., 2000) or on cognitive function (7 T MR) (Kangarlu et al., 1999).

The association between the spatial distributions of the E-field and the metabolic decreases suggests that the larger effects of EPI in the inferior occipital and frontal cortices and in superior parietal cortex are likely to reflect the higher induced *E*-field in these areas. However, there is evidence that the effects of rapidly changing magnetic fields used with TMS on neuronal activity are orientation dependent (Fox et al., 2004) and thus it is likely that the regional metabolic changes with EPI may also be influenced by the geometrical distribution of the neuronal tracts in the various cortical brain regions.

The decreases in brain glucose metabolism induced by the high frequency (1ms for the EPI readout gradient; 920 Hz) $G_z$-gradient readout are consistent with findings from repetitive TMS studies. TMS pulses induce electric currents in the brain that result in neuronal activation or inhibition as a function of the frequencies and the intensity of the stimulus (Todd et al., 2006; Ziemann et al., 1996; Paus and Barrett, 2004). Specifically, paired TMS pulses at short-intervals (intervals less than 5ms; > 200Hz) cause neuronal inhibition and those of long-intervals (intervals 8–30 ms, 10–30 Hz) cause neuronal activation (Ziemann et al., 1996; Paus and Barrett, 2004; Hallett, 2000). The decreases in the normalized metabolic measures during the EPI readout gradients could reflect the inhibitory effects of electromagnetic fields on inorganic ion transport, second messengers, neurotransmitter activity and/or neuronal metabolism and the molecular mechanism(s) merit further investigation (Sinkiewicz et al., 2005; Hogan and Wieraszko, 2004; Miyakoshi, 2005). However since these regional effects reflect normalized measures we cannot ascertain whether they reflect true decreases in metabolism rather than decrements with respect to the activity in the plane where E = 0. Moreover we can not necessarily assume that decreases in metabolism reflect inhibition of neuronal activity since inhibitory neurotransmission also requires energy utilization (Ackerman et al., 1984).

Regional changes in brain activity by EPI could be a mechanism implicated in the report of enhanced mood in depressed patients that underwent EPI-based MR spectroscopic imaging (Rohan et al., 2004). In our study of normal subjects we did not observe significant changes in mood as assessed with the positive scale from the Positive and Negative Affect Scales (PANAS) (Watson et al., 1988) between the Sham and the EPI ON conditions. This could reflect the fact that our subjects were euthymic and/or alternatively that the spatial distribution of the induced *E*-field differed between our study and that from the MR spectroscopic study (Rohan et al., 2004) since this would result in a different pattern of regional effects. Nonetheless, since therapeutic interventions that use electrical or magnetic brain stimulation such as electroconvulsive therapy (ECT) (Schmidt et al., 2008), TMS (Gershon et al., 2003) and cranial electrotherapy (DeFelice 1997; Bystrisky et al., 2008) are either being used therapeutically or proposed as therapeutic agents for the treatment of depression this highlights the importance of characterizing the effects of electrical and magnetic currents on brain activity. Imaging studies aimed at understanding the mechanism(s) of action of these interventions tend to report decreases in frontal (including cingulated) activity (review Schmidt et al., 2008), though others have reported increases (McCormick et al., 2009). The mechanisms responsible for these effects are unclear and some hypothesize that these interventions enhance mood by releasing monoamines and reducing cortical excitability (Geday and Gjedde 2009).

A limitation for this study was that we were unable to draw the arterialized blood samples required for quantification of absolute metabolism and instead relied on a simplified method for estimating metabolic rate (Logan et al., 2008). Using this method, which has been shown to provide adequate estimates of metabolic rate for baseline studies we do not observe changes in the absolute metabolic rate, which contrasts with the small but significant regional differences that we report for the normalized metabolic measures (ratio of the region's metabolism to average metabolism in the axial plane where **E** = 0). This discrepancy is likely to reflect the fact that the normalized metabolic measures are more sensitive to regional effects

than the absolute measures. This is because most of the energy utilization of the brain is required to sustain the state of consciousness in contrast to the much smaller changes associated with task-induced regional brain activation or deactivation (Gjedde, 2009; Shulman et al., 2009). Thus, normalizing regional metabolism to that of whole brain amplifies the signal that is task related. Also the normalization procedure removes the variability due to the large differences in whole brain metabolic measures between subjects, which are greater than the intrasubject variability in the regional measures, thus enhancing the statistical power to detect regional differences (Wang et al., 1994).

Another limitation is that we did not measure the E-field at the isocenter of the gradient coil but estimated the E-field in the whole imaging volume (including the isocenter). However, Glover and Bowtell (2007) used an E-field probe to measure induced E-fields during MRI and found that the E-field induced by the $G_z$ coil is null at $z = 0$ and it is extremely linear with z in the imaging volume. Thus, strong theoretical and experimental evidence support the absence of E-field at $z = 0$.

Here we report that E-field changes were linearly associated to metabolic changes, which we interpreted as indicating that the metabolic decrements were due to the E-fields. However, correlations are not sufficient to probe causality and more work is required to establish a mechanistic association.

Finally in this study even though the subjects were not told the order for the ON versus the Sham conditions we did not assess if they were able to distinguish them, which would have enabled us to ensure lack of expectation differences between conditions.

This study provides preliminary evidence that in humans EPI gradients as used in fMRI studies may affect neuronal activity (decreasing normalized metabolic activity) and that these effects are non homogeneous and dependent on the local E-field. Further studies varying the direction of the EPI gradients (left vs right and anterior vs posterior) would enable to determine if the shift in regional metabolism follows that predicted by the E fields generated in the brain with these gradients.

## Acknowledgments

We thank David Schlyer, Don Warner, Paul Vaska, Colleen Shea, Youwen Xu, Lisa Muench, Barbara Hubbard, Pauline Carter, Karen Apelskog, and Linda Thomas for their contributions. Research supported by NIH's Intramural Research Program (NIAAA).

## REFERENCES

Ackerman RF, Finch DM, Babb TL, Engel J. Increased glucose metabolism during long-duration recurrent inhibition of hippocampal pyramidal cells. J. Neurosci 1984;4:251–264. [PubMed: 6693941]

Aksoz E, Aksoz T, Bilge SS, Ilkaya F, Celik S, Diren HB. Antidepressant-like effects of echo-planar magnetic resonance imaging in mice determined using the forced swimming test. Brain Res 2008;1236:194–199. [PubMed: 18755160]

Brestmann S. The physiological basis of transcranial magnetic stimulation. Trends. Cogn. Sci 2008;12:81–83. [PubMed: 18243042]

Brooks RA, Hatazawa J, Di-Chiro G, Larson SM, Fishbein DS. Human cerebral glucose metabolism determined by positron emission tomography: a revisit. J. Cereb. Blood Flow Metab 1987;7:427–432. [PubMed: 3497163]

Bystritsky A, Kerwin L, Feusner J. A pilot study of cranial electrotherapy stimulation for generalized anxiety disorder. J. Clinical Psychiatry 2008;69:412–417. [PubMed: 18348596]

Chronik BA, Rutt BK. Simple linear formulation for magnetostimulation specific to MRI gradient coils. Magn. Reson. Med 2001;45:916–919. [PubMed: 11323819]

Crasson M, Legros JJ, Scarpa P, Legros W. 50 Hz magnetic field exposure influence on human performance and psychophysiological parameters: two double-blind experimental studies. Bioelectromagnetics 1999;20:474–486. [PubMed: 10559769]

DeFelice EA. Cranial electrotherapy stimulation (CES) in the treatment of anxiety and other stress-related disorders: A review of controlled clinical trials. Stress Medicine 1997;13:31–42.

Dolan RJ. Neuroimaging of cognition: past, present, and future. Neuron 2008;60:496–502. [PubMed: 18995825]

Fox MD, Raichle ME. Spontaneous fluctuations in brain activity observed with functional magnetic resonance imaging. Nat. Rev. Neurosci 2007;8:700–711. [PubMed: 17704812]

Fox PT, Narayana S, Tandon N, Sandoval H, Fox SP, Kochunov P, Lancaster JL. Column-based model of electric field excitation of cerebral cortex. Hum. Brain Mapp 2004;22:1–14. [PubMed: 15083522]

Friston KJ, Holmes AP, Worsley KJ, Poline J-P, Frith CD, Frackowiak RSJ. Statistical Parametric Maps in functional imaging: A general linear approach. Hum. Brain Mapp 1994;2:189–210.

Geday J, Gjedde A. Monoaminergic modulation of emotional impact in the inferomedial prefrontal cortex. Synapse 2009;63:160–166. [PubMed: 19021206]

Gjedde A. Functional brain imaging celebrates 30th anniversary. Acta. Neurol. Scand 2008;117:219–223. [PubMed: 18241299]

Gershon AA, Dannon PN, Grunhaus L. Transcranial magnetic stimulation in the treatment of depression. Am. J. Psychiatry 2003;160:835–845. [PubMed: 12727683]

Glover PM, Bowtell R. Measurement of electric fields due to time-varying magnetic field gradients using dipole probes. Phys. Med. Biol 2007;52:5119–5130. [PubMed: 17762075]

Hallett M. Transcranial magnetic stimulation and the human brain. Nature 2000;406:147–150. [PubMed: 10910346]

Harel N, Uğurbil K, Uludağ K, Yacoub E. Frontiers of brain mapping using MRI. J. Magn. Reson. Imaging 2006;23:945–957. [PubMed: 16649202]

Hogan MV, Wieraszko A. An increase in cAMP concentration in mouse hippocampal slices exposed to low-frequency and pulsed magnetic fields. Neurosci. Lett 2004;5:43–47. [PubMed: 15265587]

Jackson, JD. Classical Electrodynamics. New York: John Wiley & Sons; 1975. p. 209-268.

Kangarlu A, Burgess RE, Zhu H, Nakayama T, Hamlin RL, Abduljalil AM, Robitaille PM. Cognitive, cardiac, and physiological safety studies in ultra high field magnetic resonance imaging. Magn. Reson. Imaging 1999;17:1407–1416. [PubMed: 10609989]

Logan J, Alexoff D, Kriplani A. Simplifications in analyzing positron emission tomography data: effects on outcome measures. Nucl. Med. Biol 2007;34(7):743–756. [PubMed: 17921027]

McCormick LM, Yamada T, Yeh M, Brumm MC, Thatcher RW. Antipsychotic effect of electroconvulsive therapy is related to normalization of subgenual cingulate theta activity in psychotic depression. J. Psychiatr. Res 2009;43:553–560. [PubMed: 18851858]

Miyakoshi J. Effects of static magnetic fields at the cellular level. Prog. Biophys. Mol. Biol 2005;87:213–223. [PubMed: 15556660]

Paus T. Inferring causality in brain images: a perturbation approach. Philos. Trans. R. Soc. Lond. B Biol. Sci 2005;360:1109–1114. [PubMed: 16087451]

Paus T, Barrett J. Transcranial magnetic stimulation (TMS) of the human frontal cortex: implications for repetitive TMS treatment of depression. J. Psychiatry Neurosci 2004;29:268–279. [PubMed: 15309043]

Reivich M, Kuhl D, Wolf A, Greenberg J, Phelps M, Ido T, Casella V, Fowler J, Hoffman E, Alavi A, Som P, Sokoloff L. The [18F]fluorodeoxyglucose method for the measurement of local cerebral glucose utilization in man. Circ. Res 1979;44:127–137. [PubMed: 363301]

Rohan M, Parow A, Stoll AL, Demopulos C, Friedman S, Dager S, Hennen J, Cohen BM, Renshaw PF. Low-field magnetic stimulation in bipolar depression using an MRI-based stimulator. Am. J. Psychiatry 2004;161:93–98. [PubMed: 14702256]

Rokni-Yazdi H, Sotoudeh H, Akhondzadeh S, Sotoudeh E, Asadi H, Shakiba M. Antidepressant-like effect of magnetic resonance imaging-based stimulation in mice. Prog. Neuropsychopharmacology Biol. Psychiatry 2007;30:503–509.

Rosen BR, Buckner RL, Dale AM. Event-related functional MRI: past, present, and future. Proc. Natl. Acad. Sci. USA 1998;95:773–780. [PubMed: 9448240]

Schmidt EZ, Reininghaus B, Enzinger C, Ebner C, Hofmann P, Kapfhammer HP. Changes in brain metabolism after ECT-positron emission tomography in the assessment of changes in glucose metabolism subsequent to electroconvulsive therapy--lessons, limitations and future applications. J. Affect. Disord 2008;106:203–208. [PubMed: 17662472]

Shulman RG, Hyder F, Rothman DL. Baseline brain energy supports the state of consciousness. Proc. Natl. Acad. Sci. USA 2009;106:11096–11101. [PubMed: 19549837]

Sienkiewicz Z, Jones N, Bottomley A. Neurobehavioural effects of electromagnetic fields. Bioelectromagnetics 2005:116–126.

Sokoloff L, Reivich M, Kennedy C, Des Rosiers MH, Patlak CS, Pettigrew KD, Sakurada O, Shinohara M. The [14C]deoxyglucose method for the measurement of local cerebral glucose utilization: theory, procedure, and normal values in the conscious and anesthetized albino rat. Neurochem 1977;28:897–916.

Speer AM, Kimbrell TA, Wassermann EMD, Repella J, Willis MW, Herscovitch P, Post RM. Opposite effects of high and low frequency rTMS on regional brain activity in depressed patients. Biol. Psychiatry 2000;48:1133–1141. [PubMed: 11137053]

Stehling MK, Turner R, Mansfield P. Echo-planar imaging: magnetic resonance imaging in a fraction of a second. Science 1991;254:43–50. [PubMed: 1925560]

Todd G, Flavel SC, Ridding MC. Low-intensity repetitive transcranial magnetic stimulation decreases motor cortical excitability in humans. J. App., Physiol 2006;101:500–505.

Tomasi D. Stream function optimization for gradient coil design. Magn. Reson. Med 2001;45:505–512. [PubMed: 11241710]

Tomasi D, Xavier RF, Foerster B, Panepucci H, Tannús A, Vidoto EL. Asymmetrical gradient coil for head imaging. Magn. Reson. Med 2002;48:707–714. [PubMed: 12353289]

Volkow ND, Wang GJ, Fowler JS, Rooney WD, Felder CA, Lee JH, Franceschi D, Maynard L, Schlyer DJ, Pan JW, Gatley SJ, Springer CS Jr. Resting brain metabolic activity in a 4 tesla magnetic field. Magn. Reson. Med 2000;44:701–705. [PubMed: 11064404]

Walsh V, Rushworth M. A primer of magnetic stimulation as a tool for neuropsychology. Neuropsychologia 1999;37:125–135. [PubMed: 10080370]

Wang G-J, Volkow ND, Roque CT, Cestaro VL, Hitzemann RJ, Cantos EL, Levy AV, Dhawan AP. Functional importance of ventricular enlargement and cortical atrophy in healthy subjects and alcoholics as assessed with PET, MRI imaging and neuropsychologic testing. Radiology 1993;186:59–65. [PubMed: 8416587]

Wang GJ, Volkow ND, Wolf AP, Brodie JD, Hitzemann RJ. Intersubject variability of brain glucose metabolic measurements in young normal males. J. Nucl. Med 1994;35:1457–1466. [PubMed: 8071692]

Watson D, Clark LA, Tellegen A. Development and validation of brief measures of Positive and Negative Affect: The PANAS Scales. J. Personality Social Psychology 1988;54:1063–1070.

Worsley K, Evans A, Marrett S, Neelin P. A three-dimensional statistical analysis for CBF activation studies in human brain. J. Cereb. Blood Flow Metab 1992;12:900–918. [PubMed: 1400644]

Ziemann U, Rothwell JC, Ridding MC. Interaction between intracortical inhibition and facilitation in human motor cortex. J. Physiol 1996;496:873–881. [PubMed: 8930851]

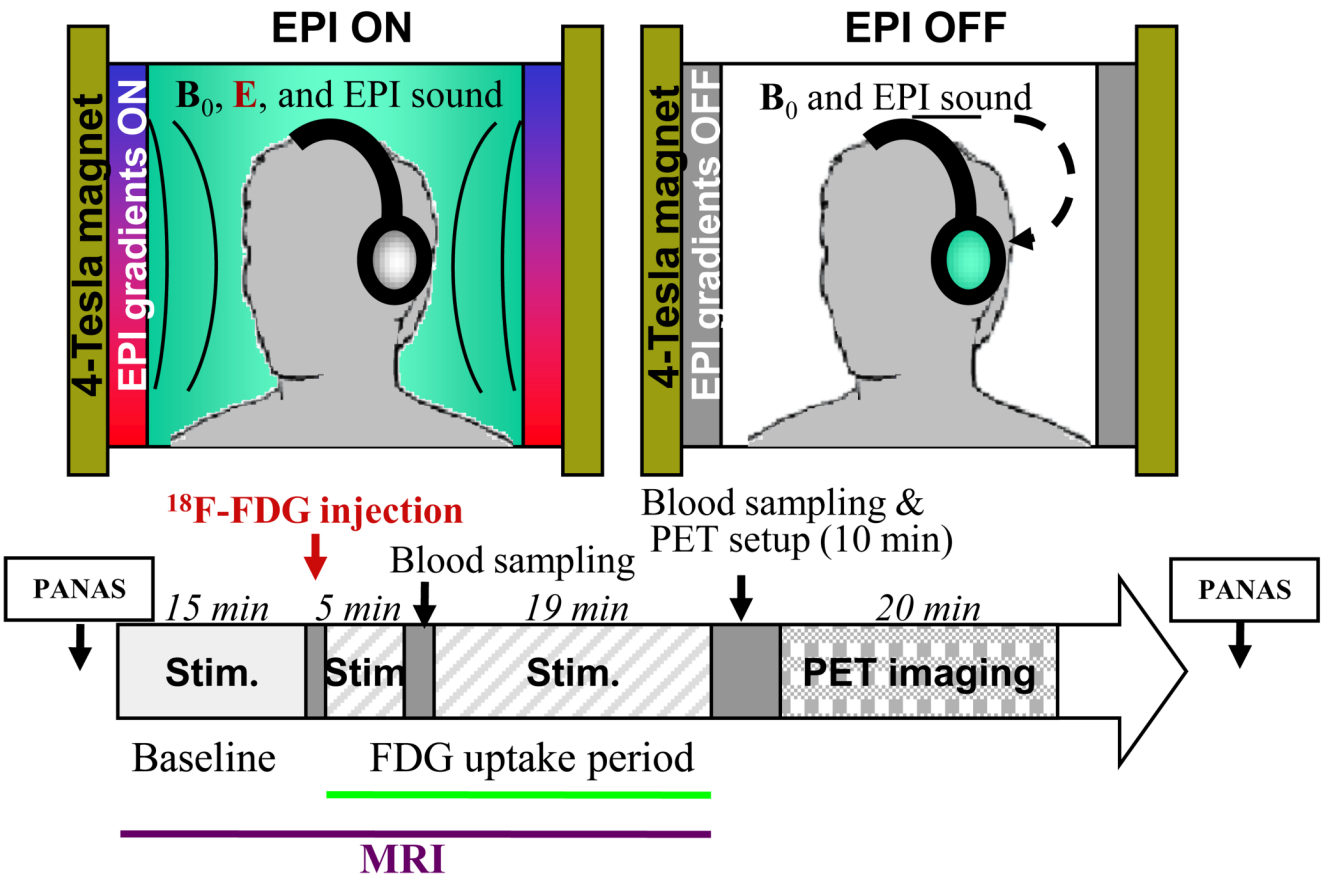


**Figure 1.**

Diagram of the experimental procedures. Subjects were tested with $^{18}$FDG and PET twice (EPI stimulation and Sham). For each of these studies the subjects remained in a 4 T MRI instrument starting 15 min. prior and during the uptake period of $^{18}$FDG (25 min. after injection) for a total of 40 min. with their heads positioned such that the center of the EPI gradients was parallel to the axial plane that transected the upper part of the corpus callosum. For the "EPI stimulation" condition they were tested with EPI gradients ON and for the "Sham" condition they were tested with the EPI gradient OFF but with exposure to the recorded auditory noise from when EPI gradients were ON. At the end of the $^{18}$FDG uptake period subjects were taken out of the MRI and positioned in the PET scanner and imaging was started 35 minutes after $^{18}$FDG injection (10 min. after they were taken out of the MRI). Blood samples were collected 5 and 30 min. after $^{18}$FDG injection to quantify radiotracer in plasma and the behavioral assessments for mood states were made using the PANAS prior to and after completion of the EPI or the Sham stimulations.

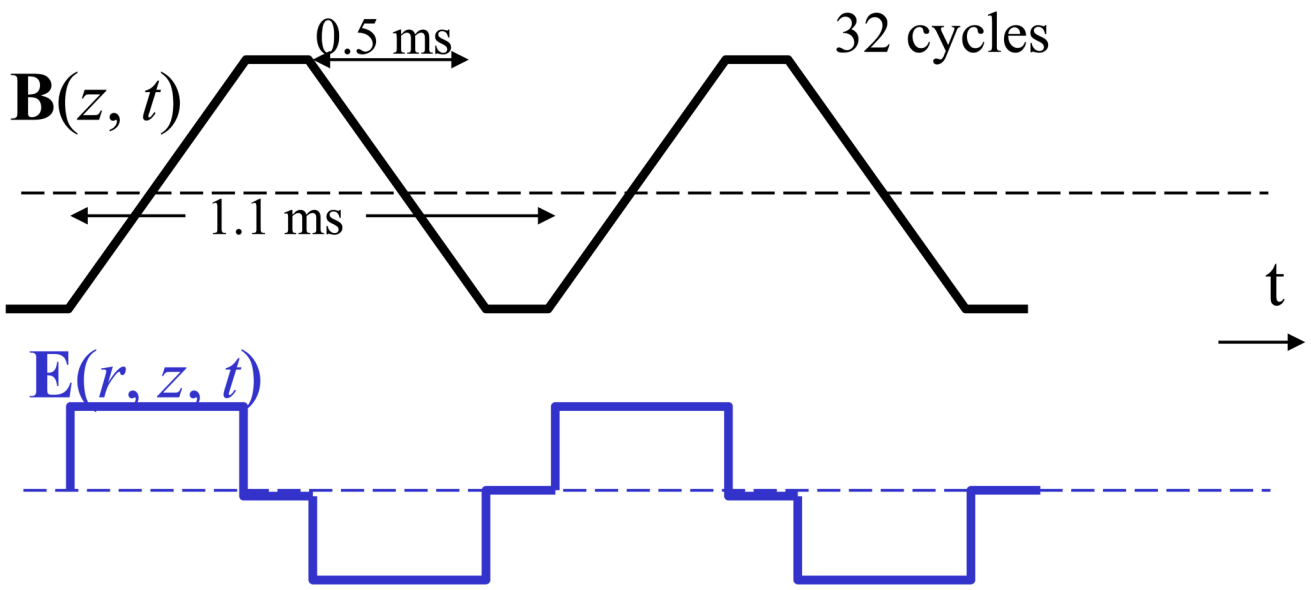


**Figure 2.**
Time-varying magnetic (B) and electric (E) fields produced by the Gz-EPI readout gradient.

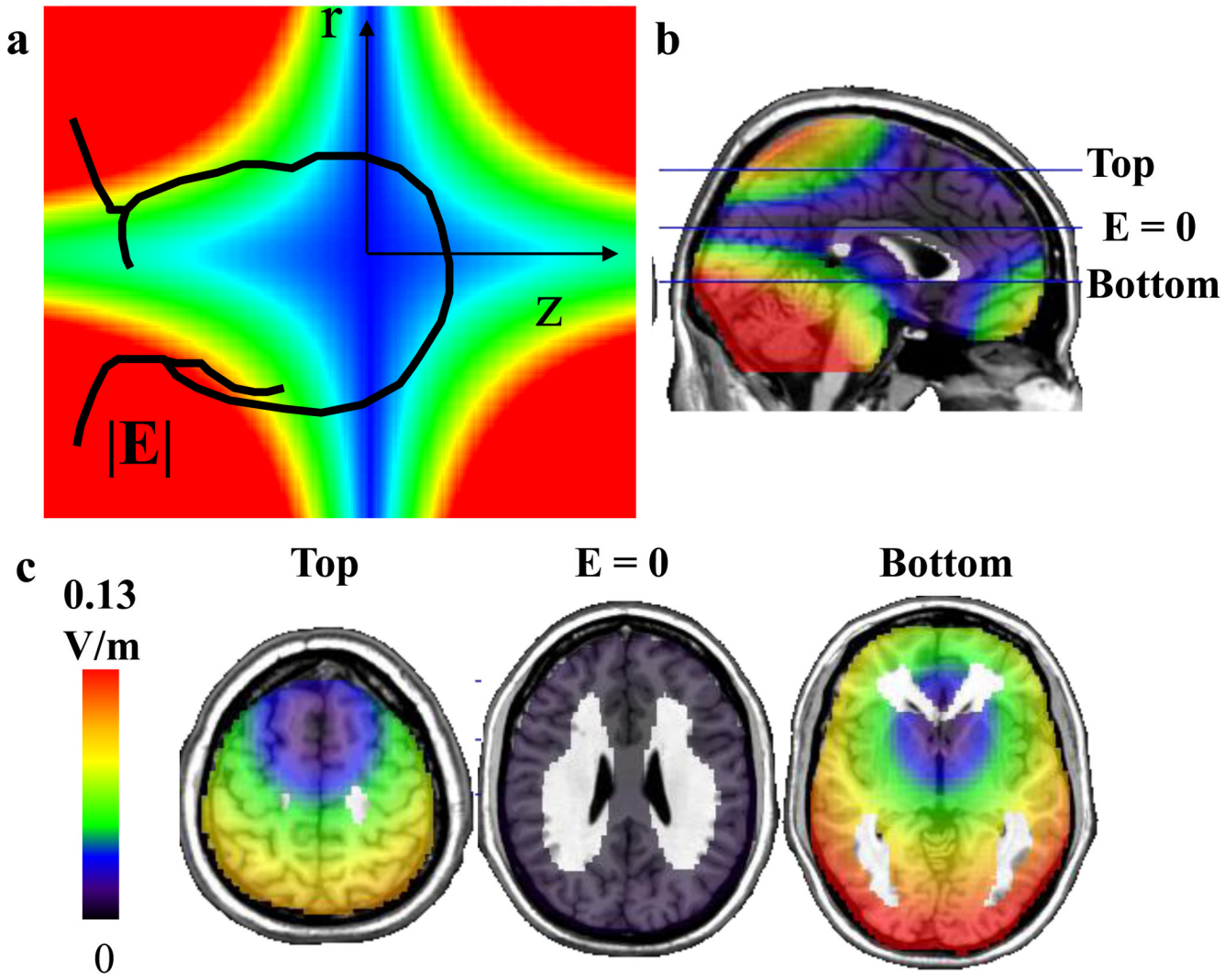


**Figure 3.**

Estimated strength of *E*-field in the brain generated by the EPI gradients. **a**. Diagram of the *E*-field induced by the EPI gradients pulses along the z-axis ($G_z$: 23 mT/m; 250 microsecond rise-time; 920 Hz), which are non-homogeneous and increase linearly from the gradient's isocenter both in the radial (r) and the z directions. **b**. Sagital plane showing the distribution of the *E*-field and location of the axial planes (top, bottom and **E** = 0) shown in panel "c". **c**. Axial planes showing the distribution of the *E*-field including the axial plane where **E** = 0. The *E*-field was strongest in the posterior and polar brain regions (top and bottom).

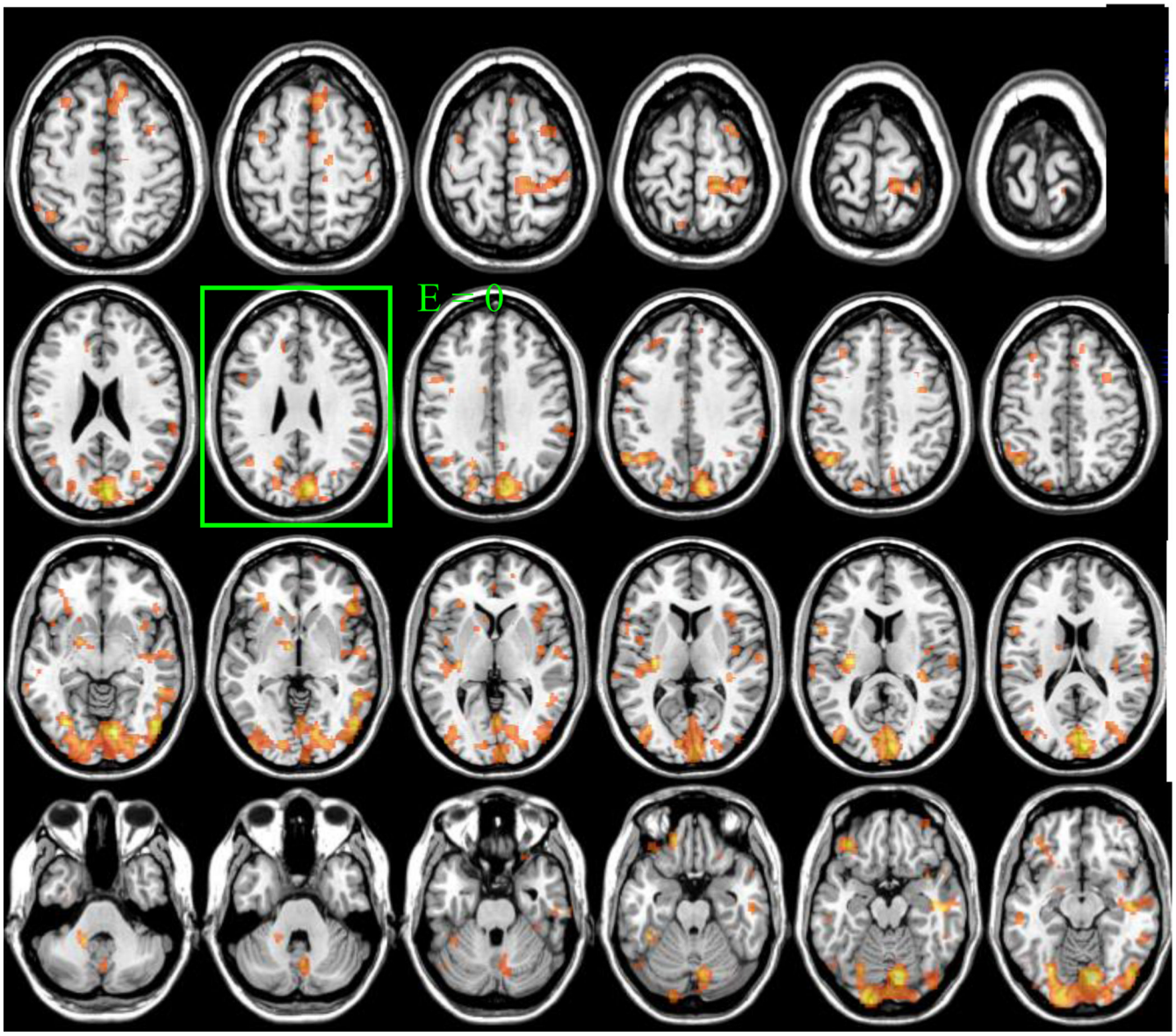


**Figure 4.**
Statistical maps showing the SPM results for the comparisons of FDG images (Sham – EPI ON) for $p < 0.05$, corrected for multiple comparisons. Brain images were normalized to the axial plane where **E** = 0.

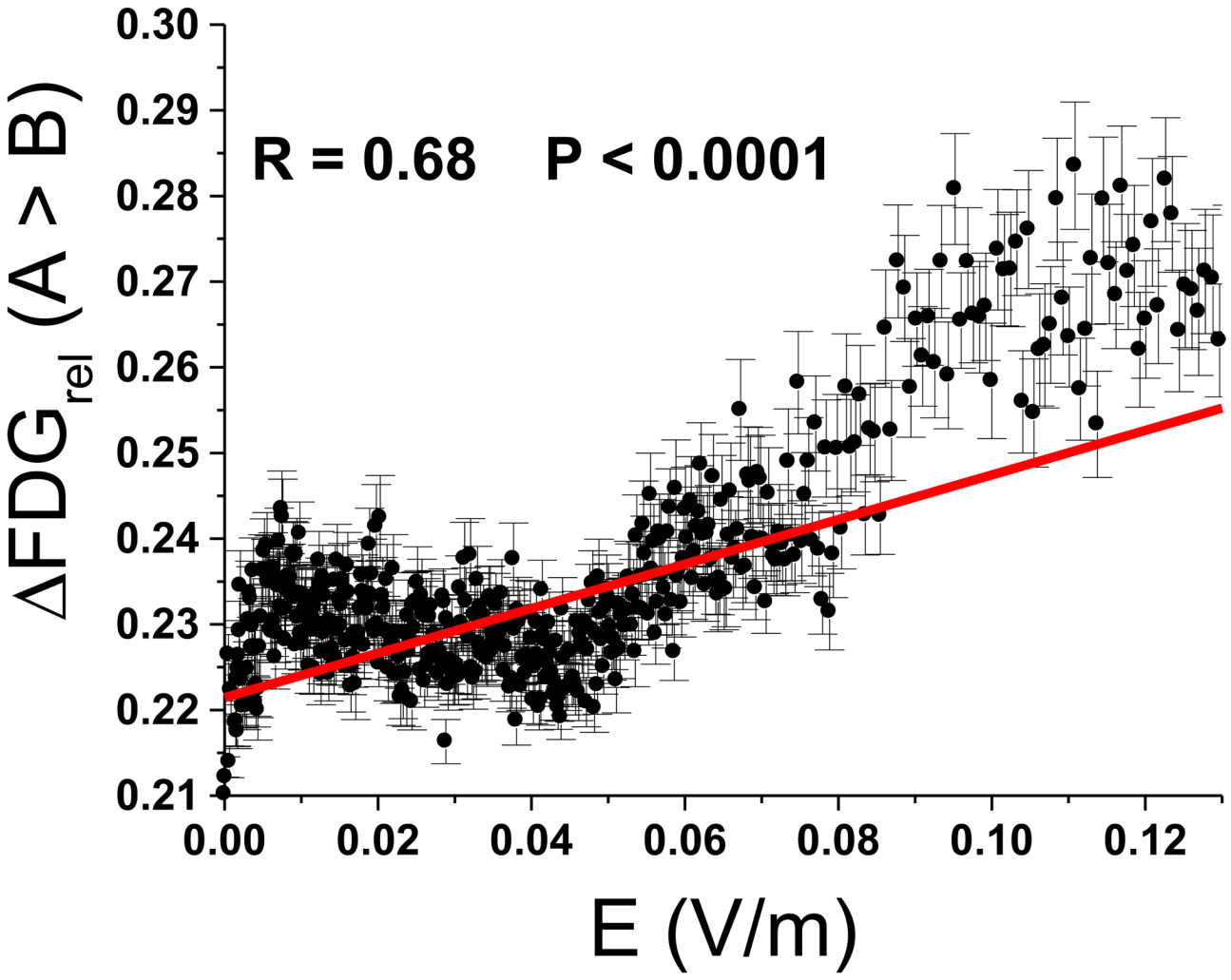


**Figure 5.**
Brain metabolic changes as a function of the local *E*-field. Diagram showing the relationship between the changes in metabolism (% change) and the strength of the local *E*-field (V/m) for voxels where SPM showed significant differences between conditions ($p < 0.05$, corrected). Regression coefficient corresponded to $r = 0.71$, $p < 0.0001$; the stronger the *E*-field the larger the decrements in metabolism.

**Table 1**

SPM Clusters where metabolism differed between EPI ON and Sham ($p < 0.05$, corrected for multiple comparisons) along with cluster size (number of voxels), significance (t value), coordinates in Talairach space (x, y z) and results for the ROI analysis showing metabolism in the corresponding anatomical area and significance for comparisons between conditions (paired t test). WM = White matter

| SPM Cluster | t | x, y, z | ON | Sham | P |
|---|---|---|---|---|---|
| 1. Inferior Occipital 8784 voxels | 7.4 | 10, −78, −12<br>−34, −70, −5 | 1.72 ±.13 | 1.62 ±.14 | 0.005 |
| 2. Left Posterior Insula 386 voxels | 5.6 | −30, −18, 10 | 1.20 ±.09 | 1.14 ±.10 | 0.05 |
| 3. Right Temporal WM 1149 voxels | 5.0 | 44, −16, −14<br>34, −32, 12<br>64, −18, 15 | 0.97 ±.08 | 0.92 ±.09 | 0.08 |
| 4. Left Inferior Frontal 450 voxels | 4.9 | −36, 36, −18<br>−32, 34, −2 | 1.54 ±.20 | 1.47 ±.18 | 0.01 |
| 5. Left Superior Parietal 720 voxels | 4.8 | −42, −58, 44 | 1.81 ±.12 | 1.76 ±.15 | 0.07 |
| 6. Right Inferior Frontal 501 voxels | 4.4 | 46, 28, 0 | 1.66 ±.12 | 1.62 ±.16 | 0.22 |
| 7. Right Superior Parietal 511 voxels | 4.1 | 18, −34, 68 | 1.48 ±.16 | 1.38 ±.15 | 0.003 |